

Fluid-induced seismicity: Pressure diffusion and hydraulic fracturing

S.A. Shapiro* and C. Dinske

Freie Universität Berlin, Fachrichtung Geophysik, Malteserstrasse 74-100, 12249 Berlin, Germany

Received January 2008, revision accepted June 2008.

ABSTRACT

Borehole fluid injections are common for the development of hydrocarbon and geothermic reservoirs. Often they induce numerous microearthquakes. Spatio-temporal dynamics of such induced microseismic clouds can be used to characterize reservoirs. However, a fluid-induced seismicity can be caused by a wide range of processes. Here we show that linear pore pressure relaxation and a hydraulic fracturing are two asymptotic end members of a set of non-linear diffusional phenomena responsible for seismicity triggering. To account for the whole range of processes we propose a rather general non-linear diffusional equation describing the pore pressure evolution. This equation takes into account a possibly strong enhancement of the medium permeability. Both linear pore pressure relaxation and hydraulic fracturing can be obtained as special limiting cases of this equation. From this equation we derive the triggering front of fluid induced seismicity, which is valid in the general case of non-linear pore pressure diffusion. We demonstrate corresponding seismicity signatures on different case studies.

INTRODUCTION

Operations involving injections of fluids from boreholes into formations are typical for the exploration and development of hydrocarbon or geothermal reservoirs. The fact that fluid injection causes seismicity has been well-established for several decades (see e.g., Pearson 1981; Zoback and Harjes 1997). Current ongoing research is aimed at quantifying and controlling this process.

Fluid induced seismicity covers a wide range of processes between the two following limiting cases. In liquid-saturated rocks with low to moderate permeability the phenomenon of microseismicity triggered by borehole fluid injections is often caused by the process of linear relaxation of pore pressure perturbations (Shapiro, Rentsch and Rothert 2005). In poro-dynamics this process corresponds to the Frenkel-Biot slow wave propagation (see Biot (1962) and an historical review by Lopatnikov and Cheng (2005), as well as an English translation of Frenkel (2005)).

In the seismic low-frequency range (hours or days of fluid injection duration) this process reduces to a linear pore pres-

sure diffusion. Fluid induced seismicity then typically shows several diffusion indicating features, which are directly related to the rate of spatial growth, to the geometry of the clouds of microearthquake hypocentres and to their spatial density (Shapiro *et al.* 2002, 2003; Parotidis, Shapiro and Rothert 2004; Shapiro, Rentsch and Rothert 2005). In some cases, spontaneously triggered natural seismicity, like earthquake swarms, also shows such diffusion-type signatures (Parotidis, Rothert and Shapiro 2003; Parotidis *et al.* 2004; Parotidis, Shapiro and Rothert 2005).

Another extreme is the hydraulic fracturing of rocks. Propagation of a hydraulic fracture is accompanied by the creation of a new fracture volume, fracturing fluid loss and its infiltration into reservoir rocks as well as diffusion of the injection pressure into the pore space of surrounding rocks and inside the hydraulic fracture (Economides and Nolte 2003). Some of these processes can be seen from features of spatio-temporal distributions of the induced microseismicity. The initial stage of fracture volume opening, as well as the back front of the induced seismicity starting to propagate after termination of the fluid injection, can be especially well identified. Shapiro and Dinske (2007), Shapiro, Dinske and Rothert (2006) and Fischer *et al.* (2008) observed these signatures in several data

*E-mail: shapiro@geophysik.fu-berlin.de

sets of hydraulic fracturing in tight gas reservoirs. The evaluation of spatio-temporal dynamics of induced microseismicity can help to estimate the important physical characteristics of hydraulic fractures, e.g., the penetration rate of the hydraulic fracture, its permeability as well as the permeability of the reservoir rock (see Shapiro *et al.* 2006; Shapiro and Dinske 2007). Therefore, understanding and monitoring of fluid-induced seismicity by hydraulic fracturing helps to characterise hydrocarbon and geothermic reservoirs and to estimate results of hydraulic fracturing

Here, we attempt to describe both types of induced microseismicity where triggering, on the one hand, is controlled by a linear pore pressure diffusion and on the other, by the process of new volume opening in rocks. We propose a general non-linear diffusional equation describing the pore pressure relaxation. This equation takes into account the possibility of a strong enhancement of the medium permeability. Both the asymptotic situations described above can then be obtained as special limiting cases of this equation. We demonstrate corresponding seismicity signatures on different real data sets.

In the following two sections we briefly review two well-understood situations of a borehole fluid-injection induced seismicity. The first one is triggering by approximately linear diffusion. The second one corresponds to triggering caused by a hydraulic fracture opening. Then we derive a non-linear diffusion equation and relate it to the phenomena considered in these two sections. Finally, we introduce one more case study and show a principally new behaviour of the triggering front.

LINEAR-DIFFUSION CONTROLLED SEISMICITY

If the injection pressure (i.e., the bottom hole pressure) is less than the minimum principal stress, then at least in the first approximation, the behaviour of the seismicity triggering in space and in time is controlled by a linear process of relaxation of stress and pore pressure perturbations initially created at the injection source. This relaxation process is described by the system of Frenkel-Biot equations for small linear deformations of poroelastic systems (Biot 1962). This equation system shows that in a homogeneous isotropic fluid-saturated poroelastic medium there are three waves propagating a strain perturbation from a source to a point of observation. These are two elastic body waves P and S (these are longitudinal and shear seismic waves) and a highly dissipative slow wave.

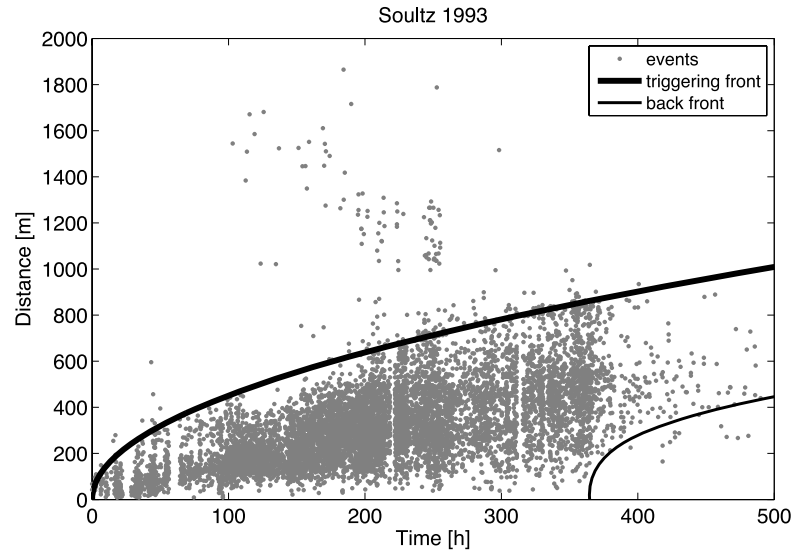
Practical experience shows that a cloud of microseismic events requires hours or even days to reach a size of several hundred metres. This process is definitely too slow to be described by the elastic wave propagation. Elastic waves in well consolidated rocks propagate in seconds over kilometre-scale distances. However, the elastic waves are primarily responsible for the elastic stress equilibration. This simple consideration immediately shows that the triggering of at least a part of the microseismic events has to be related to the slow wave. The pore pressure perturbation in the slow wave in the limit of frequencies extremely low in comparison with the global-flow critical frequency (which is usually of the order of 0.1–100 MHz for realistic geologic materials) is described by a linear partial differential equation of diffusion. It is exactly the same diffusion equation that can be obtained by uncoupling the pore pressure from the complete Frenkel-Biot's equation system in the low-frequency range. In addition, the uncoupling of the pore pressure diffusion equation requires the assumption of an irrotational solid skeleton displacement field (Detournay and Cheng 1993). In weakly heterogeneous and weakly elastically anisotropic rocks, this assumption is approximately valid. The diffusion equation describes the linear relaxation of pore-pressure perturbations in a poroelastic, fluid saturated medium.

The spatio-temporal features of the pressure-diffusion induced seismicity can be found in a very natural way from the triggering front concept (Shapiro *et al.* 2002). For the sake of simplicity we approximate a real configuration of a fluid injection in a borehole by a point source of pore pressure perturbation in an infinite, hydraulically homogeneous and isotropic fluid-saturated medium. The time evolution of the pore pressure at the injection point is taken to be a step function switched on at time 0. It is natural to assume that the probability of the triggering of seismic events increases by increasing the pore pressure perturbation. Thus, at a given time t_0 it is probable that events will occur at distances, which are smaller or equal to the size of the relaxation zone (i.e., a spatial domain of significant changes) of the pore pressure. For larger distances the events are characterized by a significantly lower occurrence probability. The surface separating these two spatial domains is the 'triggering front'. In a homogeneous and isotropic medium the triggering front r_t has the following form:

$$r_t = \sqrt{4\pi Dt}, \quad (1)$$

where t is the time from the injection start and D is the hydraulic diffusivity. Geologic media are usually hydraulically

Figure 1 Fluid-injection induced microseismicity at a borehole at Soultz, France. Points: r-t plot of induced microseismic events (the thick line is a triggering front; the thin line is a back front).



heterogeneous. Equation (1) is then an equation for the triggering front in an equivalent isotropic and homogeneous poroelastic medium with the scalar hydraulic diffusivity D . Because a seismic event is much more probable in the relaxation zone than at greater distances, equation (1) corresponds to the upper bound of the cloud of events in the plot of r versus t (so-called r-t plot). Figure 1 shows an example of such an r-t plot for an injection at the Soultz (France) geothermic site.

If the injection stops at time t_0 then the earthquakes will gradually cease to occur. For times greater than t_0 a surface can be defined that describes the propagation of a maximal pore pressure perturbation in the space. This surface (also a sphere in homogeneous isotropic rocks) separates the spatial domain which is still seismically active from the spatial domain (around the injection point), which is already seismically quiet. This surface was first described in Parotidis *et al.* (2004) and termed the back front of induced seismicity:

$$r_{bf} = \sqrt{2dDt \left(\frac{t}{t_0} - 1 \right) \ln \left(\frac{t}{t - t_0} \right)}. \quad (2)$$

Here d is the dimension of the space where the pressure diffusion occurs. For example, in the normal 3D space it is equal to 3. In a 2D fault it is equal to 2. In a 1D fracture it is equal to 1. The back front is another kinematic signature of the pressure-diffusion induced microseismicity. It is often observed on real data. In situations where the injection has produced only a very moderate or even zero impact on the permeability, the back front provides estimates of hydraulic diffusivity consistent with those obtained from the triggering front (see Fig. 1).

HYDRAULIC FRACTURING CONTROLLED SEISMICITY

During the hydraulic fracturing a fluid is injected through a perforated domain of a borehole into a reservoir rock under the bottom pressure larger than the minimum principal stress. In order to understand the main features of the induced seismicity by such an operation we apply a very simple and rough approximation of the process of the fracture growth (see for details Shapiro *et al.* 2006) resulting from a volume balance for a straight planar (usually vertical - this is the case for the real-data example given below) fracture confined to the reservoir layer. This is the so-called PKN model known from the theory of hydraulic fracturing (Economides and Nolte 2003, p. 5-15-14). Basically, the half-length r_f of the fracture (which is assumed to be symmetric in respect to the borehole) is approximately given as a function of the injection time t by the following expression:

$$r_f(t) = \frac{Q_I t}{4b_f C_L \sqrt{2t} + 2b_f w}, \quad (3)$$

where Q_I is a constant injection rate of the treatment fluid, C_L is the fluid-loss coefficient, b_f is a fracture height and w is the fracture width. The first term in the denominator describes the fluid loss from the fracture into surrounding rocks. It is proportional to \sqrt{t} and has a diffusion character. The second term, $2b_f w$, represents the contribution of the effective fracture volume and depends mainly on the geometry of the fracture's vertical cross-section. In the case of hydraulic fracturing of a formation with a very low permeability (e.g., tight gas sandstones) the fracture body represents the main permeable channel in the formation. The propagating fracture

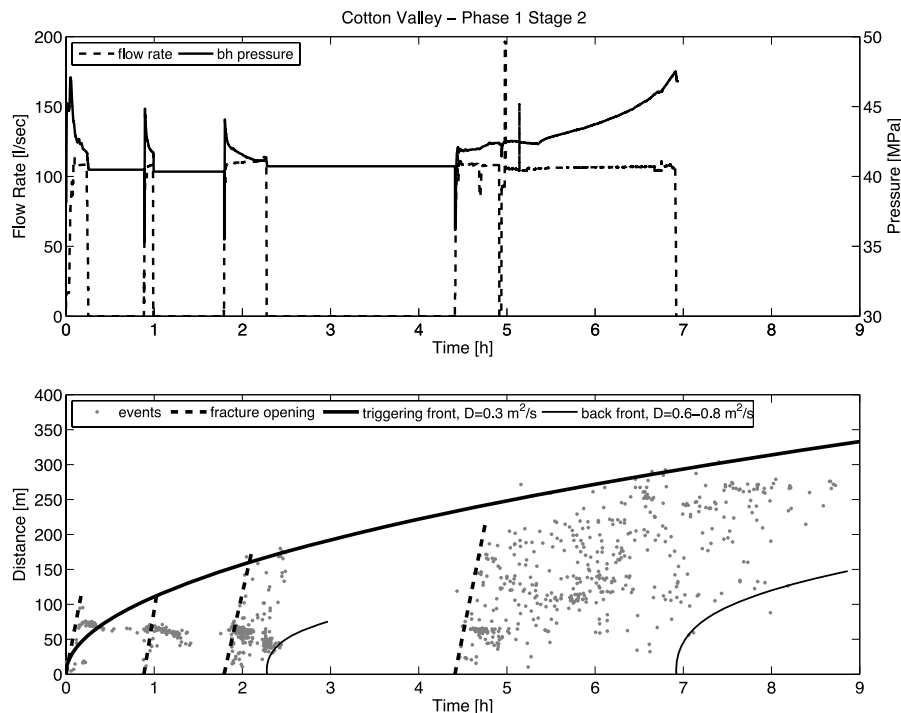


Figure 2 Hydraulic fracturing induced microseismicity at the Carthage Cotton Valley gas field (event location courtesy of James Rutledge). Top: borehole pressure (measured at the injection domain) and fluid flow rate. Bottom: r - t plot of induced microseismic events (upper parabolic line is a diffusion type approximation of the triggering; lower lines - back fronts; straight lines - fracture opening and reopening and correspondingly, linear with time triggering fronts propagation).

changes the effective stress around it and activates mainly slip events (sometimes observations of tensile events are also reported) in the critical fracture systems existing in surrounding rocks (Rutledge and Phillips 2003).

Thus, the fluid-induced microseismicity is concentrated in a spatial domain close to the hydraulic fracture. Therefore, equation (3) can be considered as a 1D approximation for the triggering front of microseismicity in the case of a penetrating hydraulic fracture (Shapiro *et al.* 2006). For a 1D hydraulic fracturing of tight rocks this equation replaces the triggering front equation (1).

During the initial phase of the hydraulic fracture growth, the process of the fracture opening is dominant. This can lead to a linear expansion of the triggering front over time. If the injection pressure drops, the fracture will close. A new injection of the treatment fluid leads to reopening of the fracture and thus, to resumption of the linear propagation of the triggering front. A long-term fluid injection leads to the domination of diffusional fluid loss processes. The growth of the fracture slows down and its size becomes approximately proportional to \sqrt{t} . After termination of the fluid injection the seismicity is mainly triggered by the process of the pressure relaxation in

the fractured domain. Correspondingly, the back front of the induced microseismicity can be observed, which is described by equation (2) with $d = 1$ (i.e., approximately, a 1D diffusion along the hydraulic fracture). Figure 2 shows an example of data demonstrating all the mentioned features of the induced seismicity during hydraulic fracturing.

SEISMICITY TRIGGERING BY NON-LINEAR DIFFUSION

Under rather general conditions, including a possible strongly non-linear interaction of the injected fluid with the rock, the pore pressure relaxation can be approximately described by a system of the two following differential equations.

The first one is the continuity equation expressing the fluid mass conservation:

$$-\frac{\partial \rho \phi}{\partial t} = \nabla \mathbf{Q} \rho, \quad (4)$$

where ρ is the density of the pore fluid, \mathbf{Q} is its filtration velocity and ϕ is the rock porosity. Note that the right-hand side of this equation describes a scalar divergence of the

filtration-velocity vector multiplied by the fluid density. Under realistic conditions the time dependent part of the quantity $\phi\rho$ is proportional to the pore pressure perturbation p : $\phi\rho = \rho_0 p S$, with ρ_0 being a reference fluid density and $S = \alpha^2(1/M_{dr} + 1/(K_{gr} - K_{dr}) + \phi(1/K_f - 1/K_{gr}))$ is a poroelastic compliance related to porosity ϕ , bulk modulus of a pore fluid K_f , bulk moduli of a grain material K_{gr} and a drained rock skeleton K_{dr} , P-wave modulus of the drained skeleton M_{dr} and the Biot-Willis effective stress coefficient $\alpha = 1 - K_{dr}/K_{gr}$ (see also Rice and Cleary 1976; Van Der Kamp and Gale 1983; Detournay and Cheng 1993).

The second equation is the Darcy law expressing the balance between the viscous friction force and the pore pressure perturbation:

$$-\mathbf{Q} = \frac{\mathbf{k}}{\eta} \nabla p, \quad (5)$$

where \mathbf{k} is the tensor of the hydraulic permeability of the rock and η is the dynamic viscosity of the pore fluid. Again, \mathbf{Q} is a vector of fluid filtration velocity. Note, that the right-hand side of this equation also contains a vector, which is resulting from a product of a permeability tensor and of a vector of gradient of pressure ∇p . In the case of non-linear fluid-rock interaction, the permeability can be a strong pressure dependent quantity. For simplicity we will neglect the anisotropy and heterogeneity of rocks. The assumption of isotropy can be lifted by rescaling and rotating the coordinate system. We are interested in situations where borehole fluid injections can be approximated by a point pore pressure source switched on at the time $t = 0$. Thus, we can consider a spherically symmetric problem and combine equations (4) and (5) in a spherical coordinate system with the origin at the injection point:

$$\frac{\partial r^2 p}{\partial t} = \frac{\partial}{\partial r} D(p) r^2 \frac{\partial}{\partial r} p, \quad (6)$$

where r is a radial distance from the injection point and we have introduced a pressure-dependent hydraulic diffusivity:

$$D(p) = \frac{k(p)\rho(p)}{S\eta\rho_0}. \quad (7)$$

The non-linear diffusion equation (6) must be completed by the initial condition of zero pore pressure perturbation before the injection starts (i.e., $p = 0$ for $t < 0$) and by the two following boundary conditions. The first condition defines the mass rate m_i of the fluid injection at the surface of an effective injection cavity of the radius R :

$$m_i(t) = 4\pi R^2 \frac{k(p)\rho(p)}{\eta} \frac{\partial}{\partial r} p \Big|_{r=R}. \quad (8)$$

The second boundary condition states a pore pressure perturbation along with its first spatial derivative vanishing at infinity faster than $1/r^2$.

Integrating equation (6) over the distance r gives:

$$\frac{\partial}{\partial t} \int_R^\infty r^2 p dr = D(p) r^2 \frac{\partial}{\partial r} p \Big|_{r=R}. \quad (9)$$

Integrating this over the time and taking into account the boundary condition at $r = R$ gives:

$$4\pi \int_R^\infty r^2 p dr = \int_0^t \frac{m_i(t)}{\rho_0 S} dt \approx \frac{1}{S} \int_0^t Q_i(t) dt. \quad (10)$$

In the last approximate part of this equation we have neglected the pressure dependency of the fluid density and introduced the volumetric rate of the fluid injection $Q_i(t)$.

In the following we will try to analyse the solution of the formulated problem without explicitly solving it. For this let us introduce the following (not very restrictive) simplifications. We will assume an injection source with a power-law injection rate $Q_i = S(i+1)Q_0 t^i$. For example, in the case of a constant rate injection source, $i = 0$ and $Q_i = SQ_0 = Q_I$ (the same injection rate as in equation (3)). We will assume a power-law dependence of the diffusivity on the pressure: $D = (n+1)D_0 p^n$. If n is large, the hydraulic diffusivity (and hence permeability) will depend strongly on the pressure. If $n = 0$, the pressure relaxation will be described by a linear diffusion equation. Finally, we will assume that the radius of the injection cavity is vanishing small (compared with the size of the microseismic cloud).

Under these assumptions equation (6) and the combined condition (10) take the following form:

$$\frac{\partial r^2 p}{\partial t} = D_0 \frac{\partial}{\partial r} r^2 \frac{\partial}{\partial r} p^{n+1}, \quad (11)$$

$$4\pi \int_0^\infty r^2 p(t, r) dr = Q_0 t^{i+1}, \quad (12)$$

where the proportionality constants D_0 and Q_0 are defined by the properties of the medium and the injection source, respectively.

To understand features of the solution of the problem stated by equations (11) and (12) we will apply the dimensional analysis (Barenblatt 1996) and especially its Π -theorem. The two equations above show that the pressure evolution depends on the following dimensional quantities, r, t, D_0 and Q_0 . They have the following physical dimensions:

$$[r] = L, \quad [t] = T, \quad [D_0] = \frac{L^2}{T P^n}, \quad [Q_0] = \frac{P L^3}{T^{i+1}}, \quad (13)$$

where L , T and P denote physical dimensions of length, time and pressure, respectively. It is clear that any 3 of the quantities r , t , D_0 and Q_0 have independent dimensions. The dimension of one of them (for example r) can be expressed in terms of the other three. In other words, only one dimensionless combination, θ , can be constructed:

$$\theta = \frac{r}{\left(D_0 Q_0^n t^{n(i+1)+1}\right)^{1/(3n+2)}}. \quad (14)$$

The following combination of quantities t , D_0 and Q_0 has the dimension of pressure:

$$\left(\frac{Q_0^2}{D_0^3 t^{(1-2i)}}\right)^{1/(3n+2)}. \quad (15)$$

Then the Π -theorem of the dimensional analysis states that the pressure must have the following form:

$$\left(\frac{Q_0^2}{D_0^3 t^{(1-2i)}}\right)^{1/(3n+2)} \Phi(\theta), \quad (16)$$

where Φ is a function that must be found by solving the problem formulated in equations (11) and (12) and the initial condition, $p = 0$ for $t < 0$.

We see that the spatial distribution of p is completely defined by the dimensionless parameter θ . If θ is large enough (i.e., small times and big distances from the source), we expect insignificant pressure increase. If θ is small (large times and small distances) a strong change of pressure must occur. Thus, a constant value of θ denotes a front of changing pressure. From the analysis of similar non-linear equations (e.g., very intensive thermal waves, see Barenblatt 1996, pp. 76–79) it is known that even a sharp front separating a zero perturbation domain from a non-vanishing perturbation values can occur. Thus a constant θ value defines the triggering front of microearthquakes r_t . From equation (14) we obtain a general result:

$$r_t \propto \left(D_0 Q_0^n t^{n(i+1)+1}\right)^{1/(3n+2)}. \quad (17)$$

Let us first assume that the diffusivity is pressure independent (this corresponds to a perfectly linear diffusion). Then $n = 0$ and $r_t \propto \sqrt{Dt}$. This corresponds to equation (1). The triggering of seismic events is controlled by a linear pore pressure relaxation. Let us now assume that n is large (this corresponds to an extremely non-linear diffusion). Then $r_t \propto (Q_0 t^{i+1})^{1/3}$. Therefore, in this case the triggering front is defined completely by the volume of the fluid injected. In other words, an opening of a new pore (or fracture) volume occurs in the spatial domain between the injection source and the triggering front. For example, in the case of a constant injection rate, $i =$

0 and $r_t \propto (Q_0 t)^{1/3}$. This is a 3-dimensional generalization of equation (3) in the small time limit (i.e., in the phase of an active linear with a time opening of a single hydraulic fracture). Therefore, we conclude that depending on the parameter n , equation (11) describes a broad range of phenomena: from a linear pore pressure relaxation to an active 3-dimensional hydraulic fracturing of the medium. This latter limiting case of non-linear diffusion will be used in the next section for an interpretation of a case study.

A CASE STUDY-BARNETT SHALE

Features of hydraulic fracturing considered in this section are defined by specific properties of the Barnett Shale gas reservoir (Fisher *et al.* 2002, 2004; Maxwell *et al.* 2006). Of course, also the features of the tectonic stress field there (which still remains to be better understood) would be of significant importance. The Barnett Shale is a marine shelf deposit from the Mississippian age. It is an organic-rich black shale with extremely low permeability on the order of 0.1–0.5 microdarcy. We have analysed the microseismic Barnett data courtesy of the Pinnacle Technology. They were obtained by hydraulic fracturing from a vertical borehole in the Lower Barnett Shale of the Fort Worth Basin. They demonstrate a typical hydraulic fracture fairway network from a vertical well in the core area of Barnett (Fisher *et al.* 2002). Figures 3 and 4 show the 3D character of the growth of the microseismic cloud. We observe an increase of the cloud size over time along all the three of its spatial dimensions.

To understand these data we propose the following simple model related to our consideration in the previous sections. We assume that a virgin reservoir rock is almost impermeable. This would lead to a negligible fluid loss from the fractured domain. Additionally, we assume that the treatment fluid is incompressible and during its injection it deforms and opens weak, compliant, pre-existing fractures in a limited volume of the rock. We will assume that the fractures can be opened if the pore pressure exceeds a given critical value p_c . We will define the perturbation of the pore pressure p relative to this critical value. As soon as a fracture has been opened, the permeability of the rock strongly increases and the fluid can be further transported to open the next fractures. Note that a fracture opening (i.e., a width) is a function of the pore pressure perturbation. However in the case of the extreme increase of permeability we can assume, approximately, that from the injection source up to the filtration front (where $p = 0$), the radial variations of the bulk porosity filled by the treatment fluid are weak. Equation (3) must then be

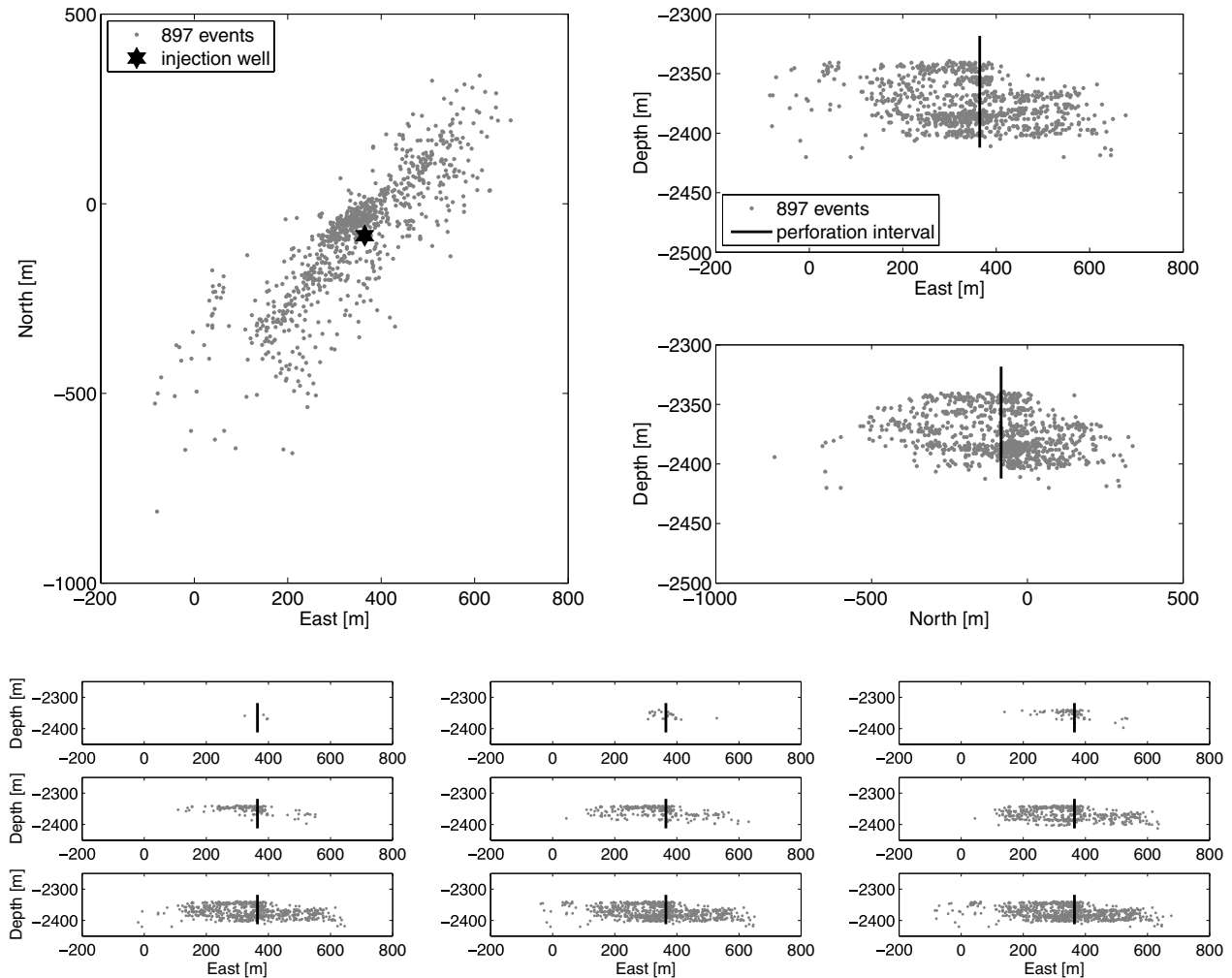


Figure 3 Hydraulic fracturing induced microseismicity in Barnett Shale (data courtesy of Shawn Maxwell, Pinnacle Technologies). Top: map and vertical plane projections of the microseismic cloud. Bottom: temporal evolution of the microseismicity on a vertical plane projection (note, that the vertical and horizontal scales are equal here).

replaced by

$$r(t) = A(Q_I t / \phi)^{1/3}. \quad (18)$$

Here $r(t)$ is the growing size of the fractured domain, ϕ is its fractured porosity filled by the treatment fluid and A is a dimensionless geometric factor equal e.g., to $1/2$ or to $(3/(4\pi))^{1/3}$ in the case of cubic or spherical fractured domains, respectively.

Therefore an r - t plot will show a $t^{1/3}$ parabolic envelope of corresponding microseismic clouds. Note, that this type of behaviour of the triggering front has been derived in the previous section from a consideration of a non-linear 3D diffusion equation with the hydraulic diffusivity very strongly

depending on the pore pressure. It corresponds to equation (17) with $i = 0$ and a large n . This type of behaviour is exactly demonstrated by the Barnett Shale data set we have at our disposal. Figure 5 shows the injection pressure, fluid rate and the r - t plot for the microseismic cloud whose different projections were given in Figs 3 and 4. One can see that the cubic root type of the triggering front describes the data significantly better than a square-root parabola.

The cubic root parabola of Fig. 5 and equation (18) permit us to estimate the porosity opened and connected by the treatment fluid. Figures 3, 4 and 5 yield an approximate estimate of this additional open porosity of the order of 0.001 per cent and the parameter A of the order of 1.

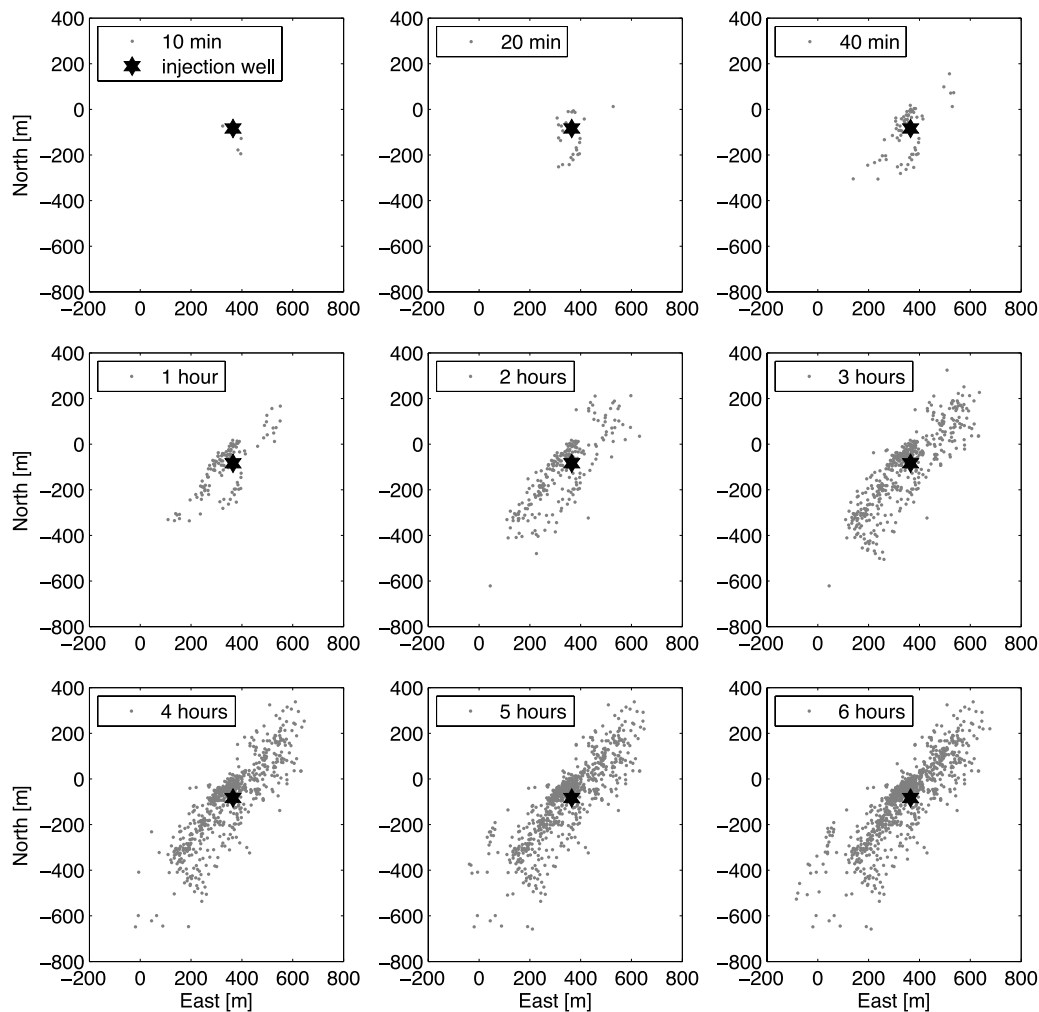


Figure 4 Hydraulic fracturing induced microseismicity in Barnett Shale (data courtesy of Shawn Maxwell, Pinnacle Technologies). Temporal evolution of the microseismicity in a map projection.

CONCLUSIONS

Understanding spatio-temporal dynamics of microseismic clouds contributes to reservoir characterization. It helps us to monitor and describe hydraulic fractures. For example, r - t -plots show signatures of fracture volume growth, fracturing fluid loss, as well as diffusion of the injection pressure into rocks and inside the fracture. Linear diffusion controlled triggering is often observed in geothermal reservoirs. Triggering controlled by volume creation is usually observed at hydraulic fracturing of tight gas reservoirs.

Here we have shown that linear pore pressure relaxation and hydraulic fracturing are two asymptotic end members of a set of non-linear diffusional phenomena responsible for seismicity triggering. We have proposed a general non-linear

diffusional equation describing the pore pressure evolution and taken into account a possibly strong enhancement of the medium permeability. Both linear pressure relaxation and hydraulic fracturing can be obtained as special limiting cases of this equation. From this equation we have derived an expression for the size of the triggering front of fluid induced seismicity, which is valid in the general case of non-linear pore pressure diffusion.

We have shown that microseismic features of hydraulic fracturing in Barnett Shale correspond to non-linear pressure diffusion in a medium with permeability very strongly enhanced by a fluid injection. It seems that the volumetric (possibly tensile) opening of preexisting fractures embedded into an extremely impermeable compliant matrix is the dominant mechanism controlling the dynamics of the induced

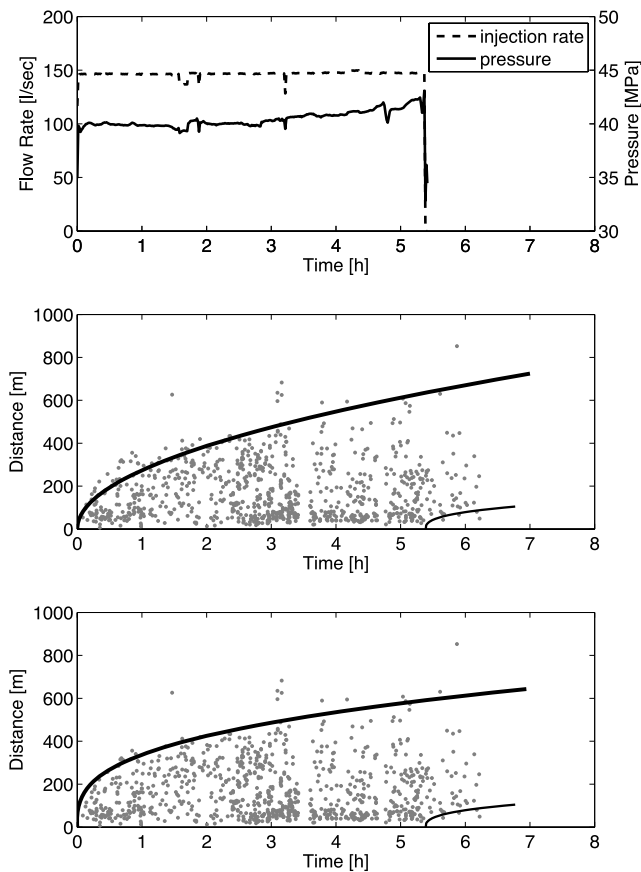


Figure 5 Hydraulic fracturing induced microseismicity in Barnett Shale (data courtesy of Shawn Maxwell, Pinnacle Technologies). Top: borehole pressure (measured at the injection domain) and fluid flow rate. Middle and bottom: the r-t plot of induced microseismic events with different envelopes (in the middle - a diffusion type approximation of the triggering ($t^{1/2}$); dashed line - a possible indication of a back front; bottom: a cubic root parabola ($t^{1/3}$) better matching the data).

microseismicity. This process can be denoted as a 3D volumetric hydraulic fracturing. The r-t plot has a characteristic cubic-root parabolic behaviour.

ACKNOWLEDGEMENTS

The work presented here has been funded by the sponsors of the PHASE university research project. The assistance of Shawn Maxwell from Pinnacle Technology in obtaining a Barnett Shale data set is greatly appreciated.

REFERENCES

Barenblatt G.I. 1996. *Scaling, Self-similarity and Intermediate Asymptotics*. Cambridge University Press. ISBN 100521435226.

- Biot M.A. 1962. Mechanics of deformation and acoustic propagation in porous media. *Journal of Applied Physics* **33**, 1482–1498.
- Detournay E. and Cheng A.H.-D. 1993. Fundamentals of poroelasticity. In: *Comprehensive Rock Engineering: Principles, Practice and Projects* (ed. J.A. Hudson), pp. 113–171. Pergamon Press.
- Economides M.J. and Nolte K.G. 2003. *Reservoir Stimulation*, 3rd edn. Wiley & Sons.
- Fisher M.K., Davidson B.M., Goodwin A.K., Fielder E.O., Buckler W.S. and Steinberger N.P. 2002. Integrating fracture mapping technologies to optimize stimulations in the barnett shale. 2002 SPE meeting, San Antonio, Texas, USA, Expanded Abstracts, SPE77411.
- Fischer T., Hainzl S., Eisner L., Shapiro S.A. and Le Calvez J. 2008. Microseismic signatures of hydraulic fracture growth in sediment formations: Observations and modeling. *Journal of Geophysical Research* **113**, B02307. doi:10.1029/2007JB005070
- Fisher M.K., Heinze J.R., Harris C.D., Davidson B.M., Wright C.A. and Dunn K.P. 2004. Optimizing horizontal completion techniques in the barnett shale using microseismic fracture mapping. 2004 SPE meeting, Houston, Texas, USA, Expanded Abstracts, SPE90051.
- Frenkel J. 2005. On the theory of seismic and seismoelectric phenomena in a moist soil. *Journal of Engineering Mechanics* **131**, 879–887.
- Lopatnikov S.L. and Cheng A.H.-D. 2005. If you ask a physicist from any country: Atribute to yacov il'ich frenkel. *Journal of Engineering Mechanics* **131**, 875–878.
- Maxwell S., Waltman C.K., Warpinski N., Mayerhofer M. and Boroumand N. 2006. Imaging seismic deformation induced by hydraulic fracture complexity. 2006 SPE meeting, San Antonio, Texas, USA, Expanded Abstracts, SPE102801.
- Parotidis M., Rothert E. and Shapiro S.A. 2003. Pore-pressure diffusion: A possible triggering mechanism for the earthquake swarms 2000 in Vogtland/nw-Bohemia, Central Europe. *Journal of Geophysical Research* **30**, 1–12. doi:10.1029/2003GL018110
- Parotidis M., Shapiro S.A. and Rothert E. 2004. Back front of seismicity induced after termination of borehole fluid injection. *Geophysical Research Letters* **31**, L02612. doi:10.1029/2003GL018987
- Pearson C. 1981. The relationship between microseismicity and high pore pressures during hydraulic stimulation experiments in low permeability granitic rocks. *Journal of Geophysical Research* **86**, 7855–7864.
- Rice J.R. and Cleary M.P. 1976. Some basic stress diffusion solutions for fluid-saturated elastic porous media with compressible constituents. *Reviews of Geophysics and Space Physics* **14**, 227–241.
- Rutledge J.T. and Phillips W.S. 2003. Hydraulic stimulation of natural fractures as revealed by induced microearthquakes, carthage cotton valley gas field, east texas. *Geophysics* **68**, 441–452.
- Shapiro S.A. and Dinske C. 2007. Violation of the kaiser effect by hydraulic-fracturing-related microseismicity. *Journal of Geophysical Engineering* **4**, 378–383.
- Shapiro S.A., Dinske C. and Rothert E. 2006. Hydraulic-fracturing controlled dynamics of microseismic clouds. *Geophysical Research Letters* **33**, L14312. doi:10.1029/2006GL026365
- Shapiro S.A., Rentsch S. and Rothert E. 2005a. Characterization of hydraulic properties of rocks using probability of fluid-induced microearthquakes. *Geophysics* **70**, F27–F34.

- Shapiro S.A., Rentsch S. and Rothert E. 2005b. Fluid-induced seismicity: Theory, modeling and applications. *Journal of Engineering Mechanics* **131**, 947–952.
- Shapiro S.A., Rothert E., Patzig R. and Rindschwentner J. 2003. Triggering of microseismicity due to pore-pressure perturbation: Permeability related signatures of the phenomenon. *Pure and Applied Geophysics – Pure and Applied Geophysics* **160**, 1051–1066.
- Shapiro S.A., Rothert E., Rindschwentner J. and Rath V. 2002. Characterization of fluid transport properties of reservoirs using induced microseismicity. *Geophysics* **67**, 212–220.
- Van Der Kamp G. and Gale J.E. 1983. Theory of earth tide and barometric effects in porous formations with compressible grains. *Water Resources Research* **19**, 538–544.
- Zoback M.D. and Harjes H.-P. 1997. Injection-induced earthquakes and crustal stress at 9 km depth at the KTB deep drilling site, Germany. *Journal of Geophysical Research* **102**, 18 477–18 491.